

Flux-Flow Resistance in Frustrated Josephson-Junction Arrays

Ying-Hong Li and S. Teitel

Department of Physics and Astronomy, University of Rochester, Rochester, New York 14627

(Received 2 July 1990)

We carry out equilibrium and steady-state simulations of a periodic square Josephson-junction array in the presence of a transverse magnetic field giving a uniform frustration of $f = \frac{2}{5}$. We find a first-order transition to the low-temperature superconducting phase. Linear resistivity above T_c and nonlinear resistivity below T_c are interpreted in terms of vortex fluctuations.

PACS numbers: 74.60.Ge, 64.60.-i, 74.50.+r, 85.25.Dq

Two-dimensional periodic arrays of Josephson junctions in a transverse applied magnetic field have been the subject of much theoretical and experimental investigation.^{1,2} The magnetic field serves to induce an ordered lattice of vortices in the ground state, analogous to the flux-line lattice in the mixed phase of a type-II superconductor.³ Fluctuations of vortex excitations play a key role in determining the nature of the phase transition and other physical properties of these systems.³⁻⁶ The study of Josephson arrays is now of renewed interest with the discovery of the high-temperature superconductors. In these type-II materials, with high T_c and large κ , great attention has recently focused on the importance of flux-line fluctuations in determining phase boundaries⁷ and resistivity due to flux flow or creep.⁸ The large anisotropy between the copper-oxide planes has suggested two-dimensional behavior in some limits.⁹ However, relevant material parameters, such as the pinning mechanisms important in flux-flow resistance, are, in general, poorly characterized. The 2D Josephson array, where geometry and all microscopic parameters are, in principle, known, can therefore serve as a useful system for studying the response of highly correlated vortices to temperature, applied currents, and magnetic fields.

The Hamiltonian for a square $L \times L$ array of Josephson junctions is³

$$\mathcal{H} = -J_0 \sum_{\langle i,j \rangle} \cos(\theta_j - \theta_i - A_{ij}), \quad (1)$$

where θ_i is the phase of the superconducting node at site i , $A_{ij} = (2e/\hbar c) \int_i^j \mathbf{A} \cdot d\mathbf{l}$ is the integral of the vector potential from node i to node j , and the bare critical current of an isolated junction is $I_0 = (2e/\hbar)J_0$. The A_{ij} obey the constraint that the sum around any unit cell of the array is a constant,

$$A_{ij} + A_{jk} + A_{kl} + A_{li} = 2\pi f,$$

where the uniform frustration $f = Ha^2/\Phi_0$ is the number of flux quanta Φ_0 of external magnetic field H per unit cell of area a^2 of the array. The induced density of vortices in the phases θ_i is equal to the frustration f . Henceforth, temperatures will be cited in units of J_0 ,

currents in units of I_0 , and distances in units of a .

Detailed equilibrium^{5,10} and dynamical^{6,11,12} studies of the model (1) have been carried out only for the simplest fractional values $f=0$, $\frac{1}{2}$, and $\frac{1}{3}$. In this work we consider the case $f = \frac{2}{5}$, which we chose as the simplest fraction which nevertheless has a relatively complicated ground-state vortex lattice. This structure is shown as the inset in Fig. 1. Since $\frac{2}{5} \approx \frac{1}{2}$, the ground state is seen to consist of striped domains of the $f = \frac{1}{2}$ -like ground state (i.e., a checkerboard pattern) separated every five cells by a domain wall.^{3,13} The ground state thus has long-range order with translational periodicity of 5 along the array axes, but a local short-range order with translational periodicity of 2. This two-scale structure may be viewed as arising from the competition between vortex-vortex interactions and the effective square periodic pinning potential implied by the array structure. Our interest is to investigate the effects of this two-scale structure on the steady-state resistive behavior. We also note here that the ground state breaks the cubic rotational symmetry of the square array by aligning the stripes along a particular diagonal direction.

We start by considering the equilibrium behavior of the model. Metropolis Monte Carlo simulations were carried out using the Hamiltonian (1) with periodic

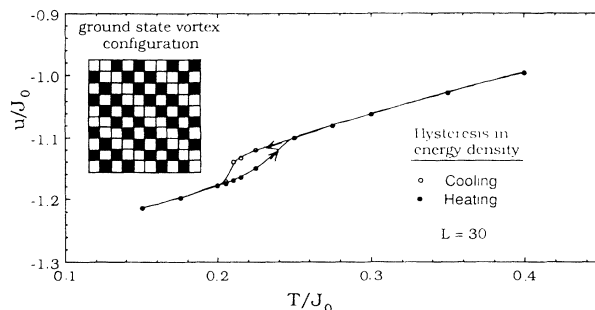


FIG. 1. Energy density u vs temperature T . Hysteresis upon successive cooling and heating indicates a first-order phase transition at $T_c \approx 0.21$. Results are for a lattice of length $L = 30$. Inset: The ground-state vortex lattice; a black square represents a unit vortex in the phases θ_i .

boundary conditions on $L=10$ to 40 square lattices. 5000 passes per site for equilibration, followed by 20000 passes per site for averaging, were used to compute the energy density u , specific heat C , and helicity modulus Y , according to standard fluctuation expressions.⁵ Two to four independent runs were used to improve statistics and estimate errors. C was found to have a narrow peak, and Y to vanish, at $T_c \approx 0.22$. Hysteresis in u upon successive cooling and heating, shown in Fig. 1, indicates a first-order, vortex-lattice-melting transition. This contrasts with the second-order transitions found previously for the $f=0$ and $\frac{1}{2}$ cases ($f=0$ has a Kosterlitz-Thouless transition due to the unbinding of neutral vortex pairs;⁴ $f=\frac{1}{2}$ has an Ising transition due to domain excitations of the doubly degenerate ground states⁵). The discontinuous jump in Y at T_c appears close to the Kosterlitz-Thouless universal value,^{4,5} as is found for $f=0$ and $\frac{1}{2}$.

We next carry out finite-temperature dynamic simulations, using the equations of motion for the resistively shunted junction model, as described in previous work on the $f=\frac{1}{2}$ case⁶ and elsewhere.^{11,12,14} We calculate the voltage drop per unit length, V (measured in units of $R_n I_0$, where R_n is the normal shunt resistance across each junction), for an applied dc current, uniformly injected and extracted from opposite sides of the array. Periodic boundary conditions are applied in the transverse direction. Our results are for a lattice of size $L=20$. Averages are computed by integrating the equations of motion over typically 40000 discrete time steps of $\Delta t \approx 0.05(2eR_n I_0/\hbar)$. An initial 5000 steps were discarded to achieve steady state. Two independent runs were made to improve statistics and to estimate errors. $T=0$ simulations yield a critical current density for the array of $I_c \approx 0.10$. In Fig. 2, we plot $R \equiv V/I$ vs T for

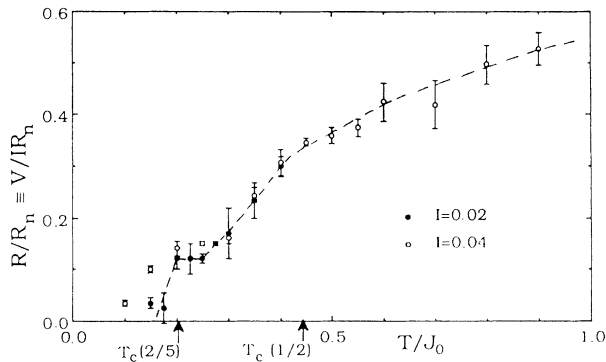


FIG. 2. Resistivity $R \equiv V/I$ vs temperature T , for values of the applied dc current, $I=0.02$ and 0.04 . The transition temperature $T_c(\frac{2}{5}) \approx 0.21$ is determined by equilibrium simulations of specific heat. The transition temperature of the $f=\frac{1}{2}$ model is shown for comparison. A plateau in R is seen for $0.2 \lesssim T \lesssim 0.3$. The dashed line is a guide to the eye only. Results are for a lattice of length $L=20$.

two values of applied current density $I=0.02$ and $0.04 < I_c$. For $T > T_c \approx 0.22$, R approaches the finite linear resistivity as $I \rightarrow 0$. For $T < T_c$, $Y > 0$ implies the absence of vortex diffusion at zero current, and hence V is a nonlinear function of I ; $R \rightarrow 0$ as $I \rightarrow 0$. In Fig. 2 this is evidenced by the strong dependence of R on finite I for $T < T_c$, with R rapidly decreasing as I gets smaller. Since the transition is first order, we expect a discontinuous drop to zero in the linear resistivity at T_c (this contrasts with the $f=0$ and $\frac{1}{2}$ cases where resistivity drops continuously to zero at T_c due to the second-order nature of the transition). In Fig. 2, at the smaller $I=0.02$, this is seen as a rapid drop in R just below T_c . At larger I , the drop becomes more gradual. Above T_c , the resistivity R shows a clear plateau up to $T \approx 0.3$ before rising to approach the normal-state resistivity at $T \sim 1$. We now interpret this plateau in terms of correlations within the disordered vortex fluid.

In Fig. 3 we plot the equilibrium ($I=0$) vortex structure function $S(\mathbf{q})$ versus \mathbf{q} along the diagonal (1,1) direction, for a lattice size $L=40$:

$$S(\mathbf{q}) = \langle \rho_{\mathbf{q}} \rho_{-\mathbf{q}} \rangle, \quad \rho_{\mathbf{q}} \equiv \frac{1}{fL^2} \sum_i (n_i - f) e^{i\mathbf{q} \cdot \mathbf{r}_i}, \quad (2)$$

where n_i is the integer vorticity cell i . For $T=0.205 < T_c$, Fig. 3(a) shows $S(\mathbf{q})$ with two δ -function peaks, corresponding to long-range order with translational periodicity of $\Delta r = 5/\sqrt{2}$ along the diagonal. This gives a

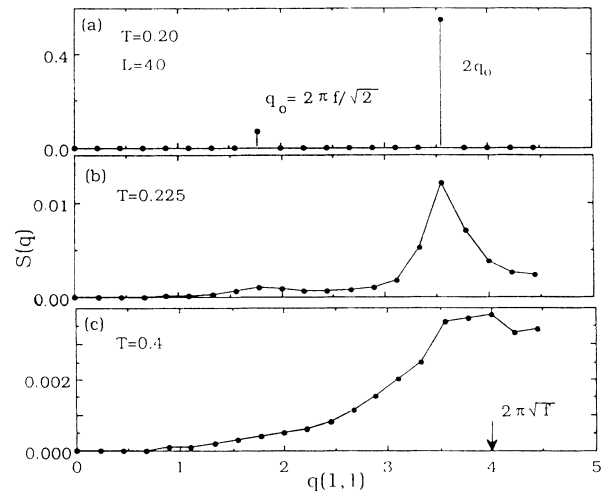


FIG. 3. Equilibrium structure function $S(\mathbf{q})$ vs \mathbf{q} along the diagonal (1,1) direction. For the finite lattice of length $L=40$, only the points $|\mathbf{q}_m| = (2\pi/L)\sqrt{2}m$, $m=0, \dots, L/2$ are computed. (a) $T=0.20 < T_c$, with two δ -function peaks indicating long-range order. (b) $T=0.225 > T_c$, in the resistivity plateau. The peaks have broadened but retain the same height ratio as in (a), indicating that ground-state order remains locally. (c) $T=0.4 \gg T_c$. The single broad peak indicates an isotropic vortex fluid. Solid lines are guides to the eye.

fundamental peak at $q_0 = 2\pi/\Delta r$, and the first harmonic at $2q_0$. At $T = 0.225 > T_c$, in the resistivity plateau, Fig. 3(b) shows these two peaks to be broadened with a finite width Δq . While this broadening signals the loss of long-range order, the continued presence of the two harmonic peaks, with the same ratio of heights, indicates that the ground-state structure persists locally on length scales $\sim \pi/\Delta q \approx 6$. As T increases above T_c , these peaks continue to broaden until they merge at $T \sim 0.3$, the end of the resistivity plateau. In Fig. 3(c) we show $S(\mathbf{q})$ for $T = 0.4$. There is now only one very broad peak, with a maximum at $q = 2\pi\sqrt{f}$, corresponding to the average vortex separation for an isotropic fluid of density f . Thus we see that correlations within the vortex fluid phase significantly affect the flux-flow resistivity of the array. The onset of linear resistivity at $T_c = 0.22$ is due to melting of the long-range order of the vortex lattice. Resistivity may be viewed as arising from the motion of domain walls separating locally ordered regions of the vortex fluid. But the rapid rise in resistivity at $T \approx 0.3$ is due to the "melting" of the local $f = \frac{1}{2}$ -like structure, yielding an isotropic vortex fluid. In this isotropic fluid, all vortices are free to move and contribute to the resistivity.

We now consider behavior below T_c . In Fig. 4(a) we show the differential resistivity dV/dI versus current I , at the temperature $T = (0.1-0.5)T_c$. dV/dI is obtained from numerical differentiation of the simulated I - V

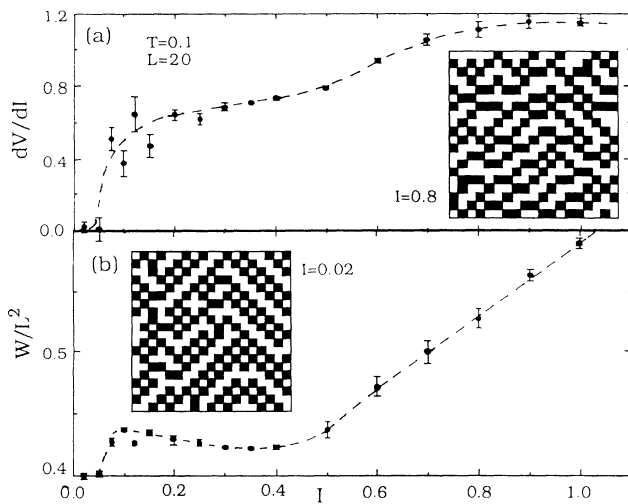


FIG. 4. (a) Differential resistivity dV/dI vs applied dc current I at temperature $T = 0.1 < T_c$. The rise to the first plateau indicates the onset of vortex flow at $I > I_c \approx 0.10$. (b) W/L^2 , the density of domain wall length between local $f = \frac{1}{2}$ -like regions, vs I . The sharp increase at $I \approx 0.5$ coincides with the second plateau in dV/dI . Dashed lines are guides to the eye only. The inset in (b) shows a snapshot of a vortex configuration in the "creep" regime at $I = 0.02 < I_c$. The inset in (a) shows a snapshot vortex configuration at high current, $I = 0.8$. Results are for a lattice of length $L = 20$.

curve. For $I < I_c \approx 0.1$, dV/dI raises rapidly from zero giving evidence of nonlinear resistivity due to thermal activation. The inset in Fig. 4(b) shows a snapshot of a vortex configuration at $I = 0.02$ in this vortex "creep" regime. It is important to note that the vortex creep here is apparently not due to simple pair unbinding (as in the $f = 0$ case), nor a rigid slipping of the ground-state lattice as a whole, as both of these processes would leave the ground-state structure largely intact. By contrast, the snapshot in Fig. 4(b) shows a much more fragmented domain structure. In particular, the cubic symmetry of the square array, which is broken by the ground state (see inset in Fig. 1), now appears restored. We have calculated an order parameter $\rho_{\mathbf{q}_0}$ [see Eq. (2)], with \mathbf{q}_0 giving the fundamental peak of Fig. 3, and find the phase of $\rho_{\mathbf{q}_0}$ to have random slips of size $2\pi f$ as a function of time, with a rate that increases with I . $\rho_{\mathbf{q}_0}$ with \mathbf{q}_0 in the perpendicular $(-1, 1)$ direction is equal in magnitude to $\rho_{\mathbf{q}_0}$ with random phase slips seemingly uncorrelated to those of $\rho_{\mathbf{q}_0}$. This suggests thermal nucleation of critical domain excitations, which cause local slips in the vortex lattice structure. Similar domain excitations have been seen in the $f = \frac{1}{2}$ and $\frac{1}{3}$ models.^{4,12}

For $I > I_c$, dV/dI levels out to a plateau, but at $I \approx 0.5$, starts to increase again. We interpret this behavior in terms of breaking of the local $f = \frac{1}{2}$ -like structure. In Fig. 4(b) we plot the wall line density W/L^2 versus I , where W is defined as the number of junctions which separate cells which are either both filled with a vortex or both empty. W measures the length of domain walls separating local $f = \frac{1}{2}$ -like structures. We see in Fig. 4(b) that, for $I_c \approx 0.1 \lesssim I \lesssim 0.5$, W is flat and only slightly higher than the $I = 0$ value. This suggests that the corresponding plateau in dV/dI is a state of freely flowing domains of the vortex lattice, due to unpinning of the domain walls. For $I \gtrsim 0.5$, W has a rapid rise, indicating a proliferation of domain walls as the local $f = \frac{1}{2}$ -like structures break up giving the increase in dV/dI . For large enough I , dV/dI must approach its asymptotic limit $dV/dI \sim R_N$. This occurs at $I \approx I_0$, the single-junction critical current, and results in the second plateau in Fig. 4(a). A snapshot of a vortex configuration at $I = 0.8$ is shown as an inset in Fig. 4(a). We have computed $S(\mathbf{q})$, Eq. (2), for $I = 0.8$, and find peaks at the same \mathbf{q} characteristic of the ground state, as in Figs. 3(a) and 3(b). However, the ratio of heights of the first harmonic to the fundamental peak is now twice what was found for the ground state. This demonstrates the breaking of $f = \frac{1}{2}$ -like structures. The vortex fluid is not isotropic, as in Fig. 3(c), since the nonzero current defines a direction. Thus, as was shown for linear resistivity R above T_c , the differential resistivity dV/dI below T_c can be viewed as a two-step process. First, one has the onset of domain flow at $I > I_c$, where the local order is that of the vortex ground-state lattice. Then one has the breaking up of local domains of $f = \frac{1}{2}$ -like structure

to give a more disordered vortex fluid. Qualitatively similar behavior in the $f = \frac{1}{3}$ model has been suggested by the simulations of Faló, Bishop, and Lomdahl.¹²

Our results suggest that local order, i.e., strong but finite-range correlations, may be more important than true long-range order in determining the size of the flux-flow resistivity. This is supported by recent experiments of Rzchowski *et al.*¹⁵ who measure $R(T)$ for frustrations $f \approx 0.52$ and 0.54 . They find a resistivity similar to $f = \frac{1}{2}$, but with a thermally activated low-temperature tail, which they attribute to the motion of defects in an otherwise $f = \frac{1}{2}$ -like vortex. Similar behavior^{15,16} is seen for very small values of f , near $f = 0$. Such considerations may be of relevance to behavior in disordered superconductors, where random pinning sites destroy¹⁷ the long-range order of the local triangular flux-line lattice.

This work has been supported by the Department of Energy under Grant No. DE-FG02-89ER14017. Computations were carried out as part of DOE sponsored research at the Florida State Supercomputer Center.

¹For recent reviews and further references, see articles in *Proceedings of the NATO Advanced Research Workshop on Coherence in Superconducting Networks*, edited by J. E. Mooij and G. B. J. Schön [Physica (Amsterdam) **152B** (1988)].

²S. P. Benz, M. S. Rzchowski, M. Tinkham, and C. J. Lobb, Phys. Rev. Lett. **64**, 693 (1990); K. H. Lee, D. Stroud, and J. S. Chung, Phys. Rev. Lett. **64**, 962 (1990); J. U. Free, S. P. Benz, M. S. Rzchowski, M. Tinkham, C. J. Lobb, and M. Octavio, Phys. Rev. B **41**, 7267 (1990).

³S. Teitel and C. Jayaprakash, Phys. Rev. Lett. **51**, 1999

(1983).

⁴For a review of the Kosterlitz-Thouless transition in arrays with $f = 0$, see J. E. Mooij, in *Advances in Superconductivity*, edited by B. Deaver and J. Ruvalds, NATO Advanced Study Institutes, Ser. B, Vol. 100 (Plenum, New York, 1983), p. 433.

⁵S. Teitel and C. Jayaprakash, Phys. Rev. B **27**, 598 (1983).

⁶K. K. Mon and S. Teitel, Phys. Rev. Lett. **62**, 673 (1989).

⁷D. R. Nelson and H. S. Seung, Phys. Rev. B **39**, 9153 (1989); A. Houghton, R. A. Pelcovits, and A. Sudbø, Phys. Rev. B **40**, 6763 (1989); E. H. Brandt, Phys. Rev. Lett. **63**, 1106 (1989).

⁸T. Nattermann, Phys. Rev. Lett. **64**, 2454 (1990); M. V. Feigel'man, V. B. Geshkenbein, A. I. Larkin, and V. M. Vinokur, Phys. Rev. Lett. **63**, 2303 (1989).

⁹P. C. E. Stamp, L. Forro, and C. Ayache, Phys. Rev. B **38**, 2847 (1988); N.-C. Yeh and C. C. Tsuei, Phys. Rev. B **39**, 9708 (1989); S. Martin, A. T. Fiory, R. M. Fleming, G. P. Espinosa, and A. S. Cooper, Phys. Rev. Lett. **62**, 677 (1989); R. S. Markiewicz, J. Phys. Condensed Matter **2**, 4005 (1990).

¹⁰W. Y. Shih and D. Stroud, Phys. Rev. B **32**, 158 (1985); G. S. Grest, Phys. Rev. B **39**, 9267 (1989).

¹¹J. S. Chung, K. H. Lee, and D. Stroud, Phys. Rev. B **40**, 6570 (1989).

¹²F. Faló, A. R. Bishop, and P. S. Lomdahl, Phys. Rev. B **41**, 10983 (1990).

¹³T. C. Halsey, Phys. Rev. B **31**, 5728 (1985).

¹⁴S. R. Shenoy, J. Phys. C **18**, 5163 (1985); R. Mehrotra and S. R. Shenoy, Europhys. Lett. **9**, 11 (1989); W. Xia and P. L. Leath, Phys. Rev. Lett. **63**, 1428 (1989).

¹⁵M. S. Rzchowski, S. P. Benz, M. Tinkham, and C. J. Lobb, Phys. Rev. B **42**, 2041 (1990).

¹⁶H. S. J. van der Zant, H. A. Rijken, and J. E. Mooij, J. Low Temp. Phys. (to be published).

¹⁷A. I. Larkin and Yu. N. Ovchinnikov, J. Low Temp. Phys. **34**, 409 (1979).